Journal of ELECTRONIC MATERIALS, Vol. 48, No. 1, 2019
https://doi.org/10.1007/s11664-018-6781-9

Electronic, Optical and Elastic Properties of $Cu_2CdGeSe_4$: A First-Principles Study

TUAN V. VU,[1,2,11] A.A. LAVRENTYEV,[3,12] B.V. GABRELIAN,[4,13] KHANG D. PHAM,[1,2,14] CHUONG V. NGUYEN,[5,15] KHANH C. TRAN,[6] HAI L. LUONG,[7] M. BATOUCHE,[8] O.V. PARASYUK,[9] and O.Y. KHYZHUN[10,16]

1.—Division of Computational Physics, Institute for Computational Science, Ton Duc Thang University, Ho Chi Minh City, Vietnam. 2.—Faculty of Electrical & Electronics Engineering, Ton Duc Thang University, Ho Chi Minh City, Vietnam. 3.—Department of Electrical Engineering and Electronics, Don State Technical University, 1 Gagarin Square, Rostov-on-Don, Russian Federation 344010. 4.—Department of Computational Technique and Automated System Software, Don State Technical University, 1 Gagarin Square, Rostov-on-Don, Russian Federation 344010. 5.—Department of Materials Science and Engineering, Le Quy Don Technical University, Hanoi 100000, Vietnam. 6.—Faculty of Materials Science and Technology, University of Science, Vietnam National University Ho Chi Minh City, 227 Nguyen Van Cu, District 5, Ho Chi Minh City, Vietnam. 7.—Department of Physics, Ho Chi Minh City University of Education, Ho Chi Minh City, Vietnam. 8.—Laboratoire de Physique Quantique et de Modélisation Mathématique, Université de Mascara, 29000 Mascara, Algeria. 9.—Department of Inorganic and Physical Chemistry, Lesya Ukrainka Eastern European National University, 13 Voli Avenue, Lutsk 43025, Ukraine. 10.—Frantsevych Institute for Problems of Materials Science, National Academy of Sciences of Ukraine, 3 Krzhyzhanivsky Street, Kiev 03142, Ukraine. 11.—e-mail: vuvantuan@tdtu.edu.vn. 12.—e-mail: alavrentyev@dstu.edu.ru. 13.—e-mail: boris.gabrelian@gmail.com. 14.—e-mail: phamdinhkhang@tdtu.edu.vn. 15.—e-mail: chuongnguyen11@gmail.com. 16.—e-mail: khyzhun@ipms.kiev.ua

Using the augmented plane wave + local orbitals method with different approximation functionals, we investigate systematically the electronic, optical and elastic properties of stannite-type $Cu_2CdGeSe_4$. Among different approximation functionals, the modified Becke–Johnson (mBJ) potential with Hubbard-corrected parameter U (mBJ + U) gives the most reliable results on the electronic properties of $Cu_2CdGeSe_4$ in comparison with the experimental data. Elastic modulus, elastic constants and the Poisson's ratio of $Cu_2CdGeSe_4$ were calculated using the Elastic software package. Optical properties such as wide spectrum of absorbed photon energy, namely 1.3–27.2 eV, high absorption coefficient (above 10^4 cm^{-1}) and optical anisotropy suggest the application of $Cu_2CdGeSe_4$ in solar cells.

Key words: Optical materials, *ab initio* calculations, electronic structure, optical properties, elastic properties

INTRODUCTION

Recently, the chalcogenide compounds of Cu_2-B^{II}-C^{IV}-X_4 (where B^{II} = Mn, Fe, Co, Ni, Zn, Cd, Hg; C^{IV} = Se, Ge, Sn; X = S, Se) are used widely in many scientific and industrial fields such as photovoltaics, optoelectronics, nonlinear optics, and photocatalysts for water splitting, due to outstanding optical and electrical properties.[1–6] Two types of the crystal structures of Cu_2-B^{II}-C^{IV}-X_4 are known to exist, namely stannite (ST) and wurtzite types, which correspond to the tetragonal and orthorhombic crystal systems.[4]

As a representative of the Cu_2-B^{II}-C^{IV}-X_4 group, the chalcogenide compound $Cu_2CdGeSe_4$ has attracted great scientific interest. For example,

(Received August 17, 2018; accepted October 30, 2018; published online November 8, 2018)

Gulay et al.[7] studied the dependence of the crystal structure and phase transformation in $Cu_2CdGeSe_4$ upon heat treatment. Accordingly, if a $Cu_2CdGeSe_4$ sample is synthesized at 1173 K adopting regular cooling to 673 K at a rate of 15 K/h and quenching in cold water, high-temperature (HT) HT-$Cu_2CdGeSe_4$ phase possessing an orthorhombic structure with unit-cell parameters a = 8.0968, b = 6.8929 and c = 6.6264 Å is obtained.[7] On the other hand, if the sample is cooled to 673 K at a rate of 10 K/h with its further annealing for 250 h, it is possible to obtain low-temperature (LT) LT-$Cu_2CdGeSe_4$ phase which has a tetragonal structure with unit-cell parameters a = 5.7482, c = 11.0533 Å.[7] Li et al.[8] studied the electronic and optical properties of $Cu_2CdGeSe_4$ in a ST phase using density functional theory (DFT) calculations in the form of generalized gradient approximation (GGA). The authors reveal that the lattice constants are in good agreement with experimental data. However, the band gap value obtained using the GGA functional is equal to 0.017 eV which underestimates the experimental value of 1.27 eV.[9] Brik et al.[10] studied the electronic and optical properties of $Cu_2CdGeSe_4$ based on DFT calculations using GGA and local density approximation (LDA) functionals. The use of these functionals yields inaccurate calculated values of the band gap (0.020 eV for GGA and 0.032 eV for LDA). The authors[10] used a scissor correction of 1.27 eV to match the experimental value to get the correct value of the band gap as well as the optical characteristics.[9] Ocheretova et al.[11] investigated the electronic structure of $Cu_2CdGeSe_4$ by x-ray emission spectroscopy (XES) and x-ray photoelectron spectroscopy (XPS). These results indicated that the top and bottom of the valence band are mainly composed from the contributions of Cu 3*d* and Cd 4*d* states, whereas the middle and upper portions of the valence band are composed from the contributions of Ge 4*p* and Se 4*p* states. Recently, Zhang et al.[12] adopted a modified Becke–Johnson (MBJ) potential with the Hubbard-corrected parameter U (mBJ + U) to evaluate the bandgap energy of two possible crystal structures in which the $Cu_2CdGeSe_4$ chalcogenide is expected to be synthesized, namely ST and kesterite (KS) types. In particular, the theoretical bandgap energies as evaluated by Zhang et al.[12] are 1.13 eV and 1.07 eV for KS-$Cu_2CdGeSe_4$ and ST-$Cu_2CdGeSe_4$, respectively, and are in good agreement with the experimental value E_g = 1.27 eV measured for this chalcogenide.

Although the electronic structure and optical properties of $Cu_2CdGeSe_4$ were studied by theoretical calculations,[8,10] some calculated parameters such as the band gap value and dielectric function parameters do not agree with the experimental findings.[7,11] This discrepancy is explained by the use of GGA and LDA functionals in the *ab initio* calculation by Li et al.[8] and by Brik et al.[10] that are not fit for such kind of compounds. So, in this study, we use a variety of density functionals to simulate the structural, electronic and optical properties of the $Cu_2CdGeSe_4$ compound. Comparing the calculated results with the experimental data we can determine the suitable density functional in DFT calculations, in particular for $Cu_2CdGeSe_4$, and in general for the quaternary chalcogenide compounds Cu_2-B^{II}-C^{IV}-X_4. In addition, using the suitable functional, we systematically study the structural, electronic, optical and elastic properties of $Cu_2CdGeSe_4$. In fact, in the present study, we reveal that the best agreement of the theoretical total density of states (DOS) curves with respect to the experimental XPS valence band spectrum is observed when we use the mBJ + U approach proposed for the first time by Zhang et al.[12] to evaluate the theoretical E_g value for $Cu_2CdGeSe_4$ in two possible structure types. However, the main optical constants and elastic properties as well as total DOS and partial DOS (PDOS) have not been studied by Zhang et al.[12] Furthermore, elastic properties of $Cu_2CdGeSe_4$ are elucidated for the first time in the present work based on first-principles band structure calculations.

COMPUTATIONAL METHODOLOGY

Based on the experimental data by Gulay et al.[7] on the structure of LT-$Cu_2CdGeSe_4$, we built a crystal model with a three-dimensional periodic scheme in which Cd, Cu, Ge and Se atoms occupy the 2a, 4d, 2b and 8i Wyckoff sites corresponding to the coordinates as following: (0, 0, 0); (1/2, 0, 1/4); (0, 0, 1/2); (0.2705, 0.2705, 0.1337) (Fig. 1). The

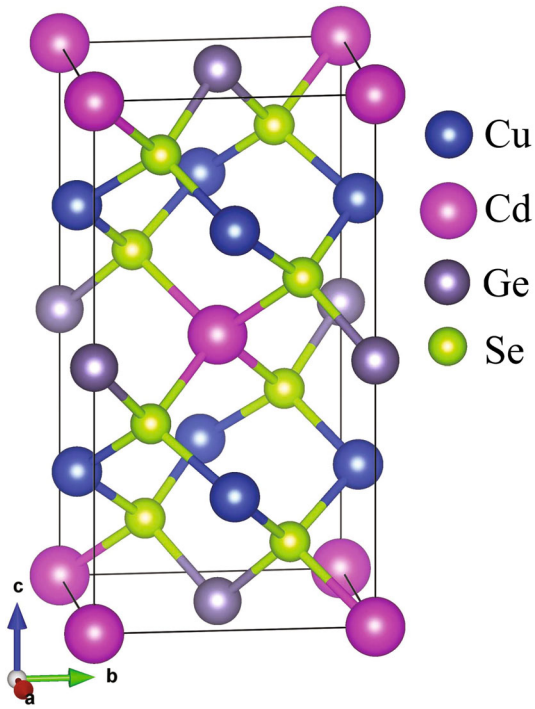

Fig. 1. Crystal structure of $Cu_2CdGeSe_4$.

stacking of the XSe_4 tetrahedra (X = Cu, Cd, Ge) in the $Cu_2CdGeSe_4$ structure is shown in Fig. 2a, while the layers viewed down the b-axis are presented in Fig. 2b. Each Cu, Cd and Ge atom is bonded to three Se atoms with different bonding lengths (Fig. 3). The unit cell parameters are a = 5.7482(2) Å and c = 11.0533(3) Å.[7]

In this study, we perform *ab initio* calculations of the electronic and optical properties of $Cu_2CdGeSe_4$ using the augmented plane wave + local orbitals (APW + lo) method as incorporated in the WIEN2k package.[13] In this method, all core, semi-core and valence electrons of atoms are taken into account in the DFT calculations. The minimum radii of the muffin-tin spheres values (R_{MT}) are set for the $Cu_2CdGeSe_4$ compound as 2.32 a.u. for Cu, 2.50 a.u. for Cd, 2.24 a.u. for Ge and 2.21 a.u. for Se (1 a.u. = 0.529177 Å). The valence configurations of Cu, Cd, Ge and Se atoms used are $3p^6 3d^{10} 4s^1$, $4p^6 4d^{10} 5s^2$, $3d^{10} 4s^2 4p^2$ and $4s^2 4p^4$, respectively. The $R_{\min}^{MT} k_{\max}$ convergence parameter is set to be equal to 7.0. Further, the valence wavefunctions inside the muffin-tin spheres are expanded till $l_{\max}$ = 10, while outside the muffin-tin spheres, till $l_{\max}$ = 4. For calculation of the exchange–correlation energy, we used the Perdew–Burke–Ernzerhof (PBE) functional[14] within the GGA approximation,[15,16] the modified Becke–Johnson (mBJ) functional[17,18] and the Yukawa screened PBE functional (in its unscreened version, YS-PBE0[19]). Besides, the corrected Hubbard parameter U[20,21] was used to increase the binding energy of d electrons and thereby to obtain the best fit between the energy position of the calculated d bands and the corresponding features of the experimental XPS spectrum.

The integration through the Brillouin zone (BZ) uses the tetrahedron method by Blochl et al.[22] and was performed on a grid of 1000 k points within the irreducible wedge of the zone. The accomplished charge density convergence of the iteration process was at least 0.0001.

It is well known that the dielectric function is a basis for solid-state spectroscopy.[23] The linear optical susceptibility of crystals can be obtained from the components of the imaginary part of the dielectric function. Calculation of the real and imaginary parts of the dielectric function and the functionals associated with it, such as the absorption coefficient, refractive index, extinction coefficient, electron energy-loss spectrum, and optical reflectivity, were described in detail in our previous study.[24]

To study elastic properties, we have created 21 different deformation structures of $Cu_2CdGeSe_4$ from the original model with a strain in the range from − 0.05 to 0.05. The independent elastic constants of $Cu_2CdGeSe_4$ (C_{11}, C_{12}, C_{13}, C_{33}, C_{44} and C_{66}) were calculated based on the second-order derivative $E''(\eta)$ of the polynomial fit $E = E(\eta)$ of energy versus strain at zero strain $\eta = 0$ using the Elastic software package[25]:

$$c_{\alpha\beta} = \frac{1}{V_0} \frac{\partial^2 E}{\partial \eta_\alpha \eta_\beta}\Big|_{\eta=0} \quad (1)$$

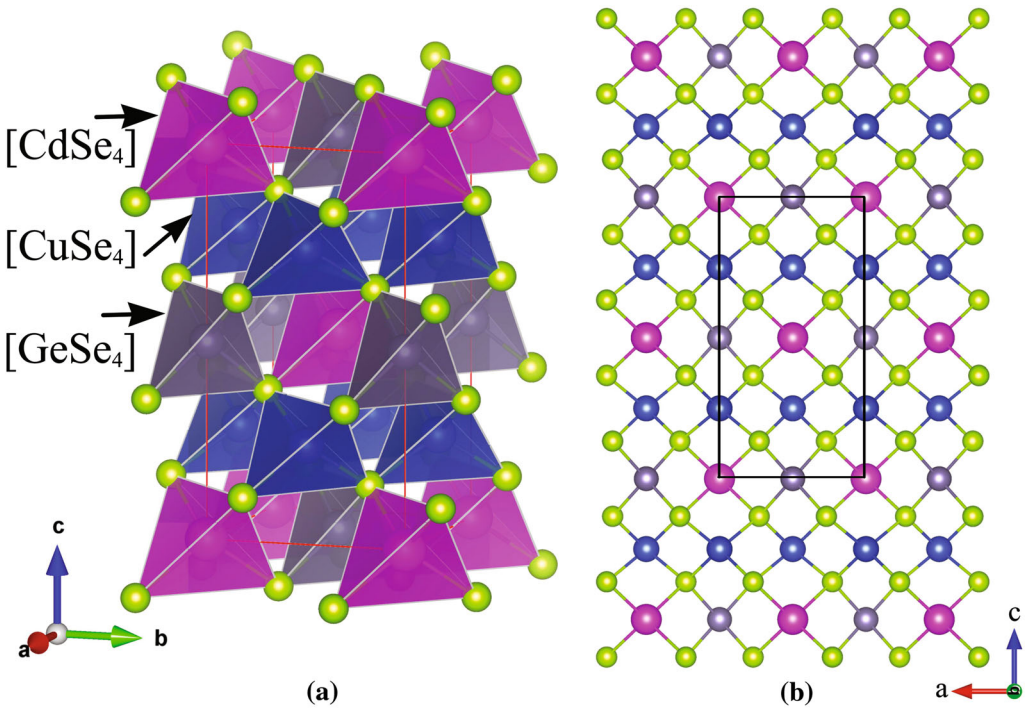

Fig. 2. (a) The stacking of the $CuSe_4$, $CdSe_4$ and $GeSe_4$ tetrahedra and (b) the structure of layers viewed down the *b*-axis in the $Cu_2CdGeSe_4$ compound.

where α, β are indices showing the types of elastic deformations in a crystal; V_0 is the volume of the crystal; η_α, η_β are the deformations in different directions of the Cartesian coordinate system. The bulk modulus B and shear modulus G were calculated from the elastic constants by the Voight–Reuss–Hill (VRH) approximation.[26,27] In accordance with the results by Hill,[26,27] the Voigt and Reuss assumptions result in the theoretical maximum and minimum values of the isotropic elastic moduli, respectively. Using energy considerations, Hill proved[26,27] that the Voigt and Reuss equations represent upper and lower limits of the true elastic constants, and recommended that a practical estimate of the bulk and shear moduli were the arithmetic means of the extremes. Hence, the average elastic moduli of an anisotropic single crystal can be approximated by Hill's average.[26,27] Note that for the tetragonal structure ($I\bar{4}2m$) $C_{13} = C_{23}$; $C_{11} = C_{22}$; $C_{44} = C_{55}$. Young's modulus E and Poisson's ratio are calculated according to the values of B and G:

$$E = \frac{9BG}{3B + G} \tag{2}$$

$$\upsilon = \frac{3B - 2G}{2(3B + G)} \tag{3}$$

RESULTS AND DISCUSSION

Structural Properties

To investigate the structural and electronic properties of the $Cu_2CdGeSe_4$ compound, we first relax its structure to obtain the lattice parameters. After full relaxation, the optimized lattice parameters of the $Cu_2CdGeSe_4$ compound are a = 5.6056 Å and c = 10.7336 Å which are in good agreement with the experimental values a = 5.7482 Å and c = 11.0533 Å[7] as listed in Table I. It can be seen that the computational method used in the present study is reasonable, and thus will be used in all following calculations.

Electronic Properties

The total DOS curves of $Cu_2CdGeSe_4$ using different approximations are presented in Fig. 4, and are compared to XPS valence band spectrum

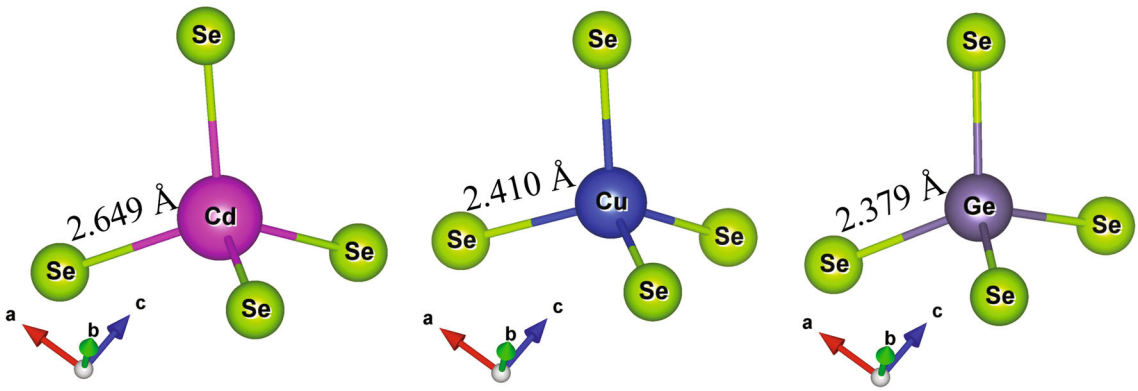

Fig. 3. Distorted $CuSe_4$, $CdSe_4$ and $GeSe_4$ tetrahedra in the $Cu_2CdGeSe_4$ structure.

Table I. The lattice constants and the atomic positions of the $Cu_2CdGeSe_4$ compound after geometric optimization

Cell parameters (Å)	***a***	***c***
This work	5.6056	10.7336
Exp.[7]	5.7482	11.0533
Other works	5.75216[a], 5.8008[b], 5.6462[b]	10.9454[a], 11.0845[b], 10.8429[b]

Atoms	***x***	***y***	***z***	***x* optim.**	***y* optim.**	***z* optim.**
Atomic positions						
Cu	0.5	0	0.25	0.5	0	0.25
Cd	0	0	0	0	0	0
Ge	0	0	0.5	0	0	0.5
Se	0.2705	0.2705	0.1337	0.2674	0.2674	0.13704

[a]Ref. 8. [b]Ref. 10.

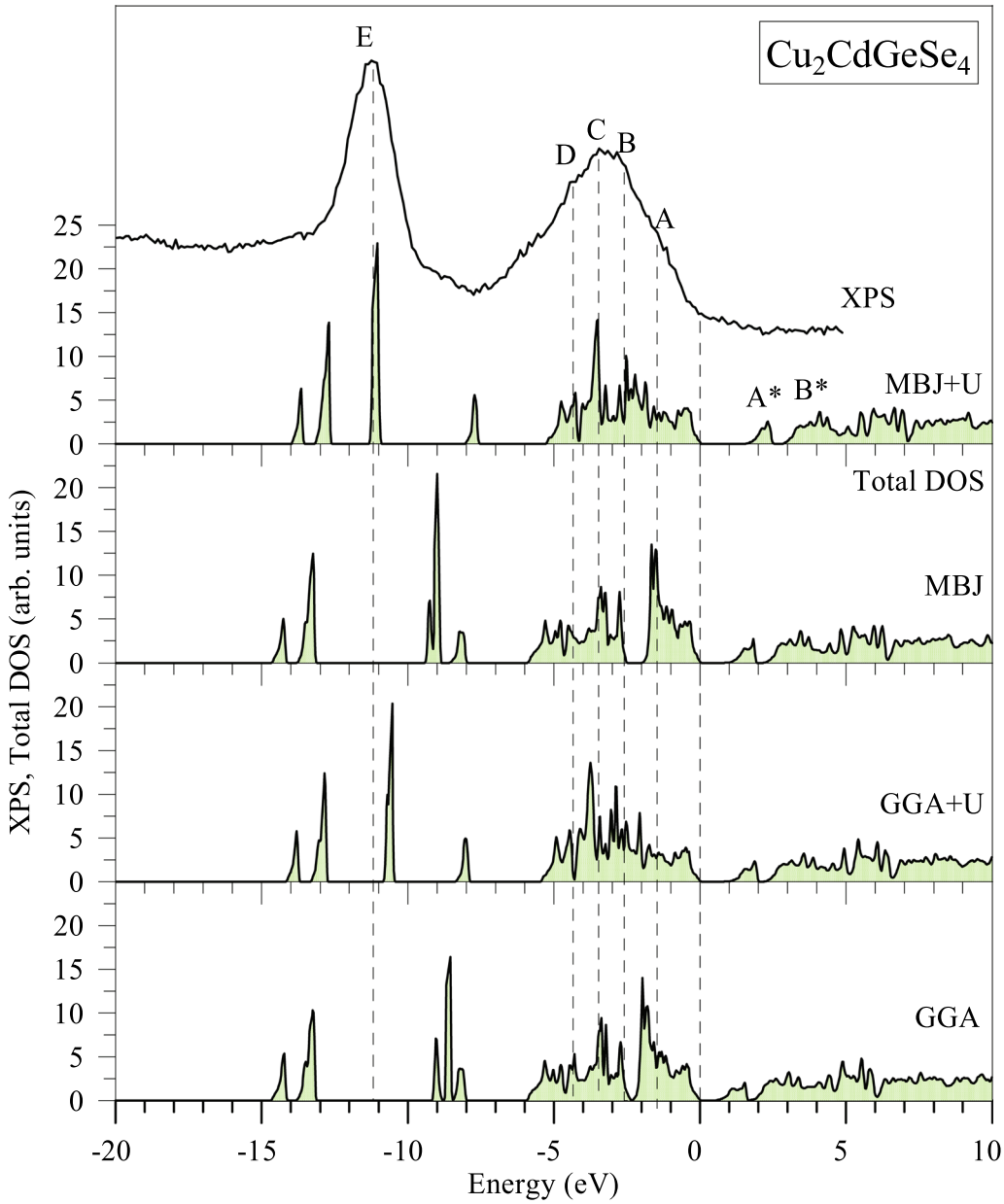

Fig. 4. Total DOS of the $Cu_2CdGeSe_4$ compound given by the GGA, GGA + U, mBJ and mBJ + U methods as compared to its XPS valence band spectrum measured in Ref. 11.

measured following the technique.[11] We find that the fit of total DOS peculiarities calculated in our work in comparison to the XPS spectrum curve increases in the following order: GGA, mBJ, GGA + U and mBJ + U. Specifically, the energy positions of the peaks of the total DOS curve given by the mBJ + U method almost coincide with those detected on the XPS spectrum curve. This confirms the correctness of the choice of the mBJ + U approximation for the exchange–correlation potential and the value of U = 0.4 Ry for Cu 3*d* electrons and U = 0.5 Ry for Cd 4*d* electrons in the DOS calculations of $Cu_2CdGeSe_4$.

Figure 5 presents the calculated PDOS of the $Cu_2CdGeSe_4$ compound within the mBJ + U method. One can observe that top and bottom parts of the valence band are mainly contributed from Cu 3*d* and Cd 4*d* states. Additionally, the upper part of the valence band is mainly contributed by hybridization between Cu 3*d*, Ge 4*p* and Se 4*p* states, forming the energy peaks C (− 3.50 eV) and B (− 2.53 eV), whereas the peak E with the energy of − 11.15 eV is mainly populated by hybridization between Cd 4*d*, Ge 4*d* and Se 4*s* states. On the right side of the Fermi energy, as shown in Fig. 5, the major contributions of Cu 4*s*, Ge 4*s* and Se 4*p* states to the conduction band with peaks A* (2.32 eV) and B* (4.12 eV) are observed. Hybridization of these electronic states at peaks B, C and E demonstrates the combination of covalent and ionic components in

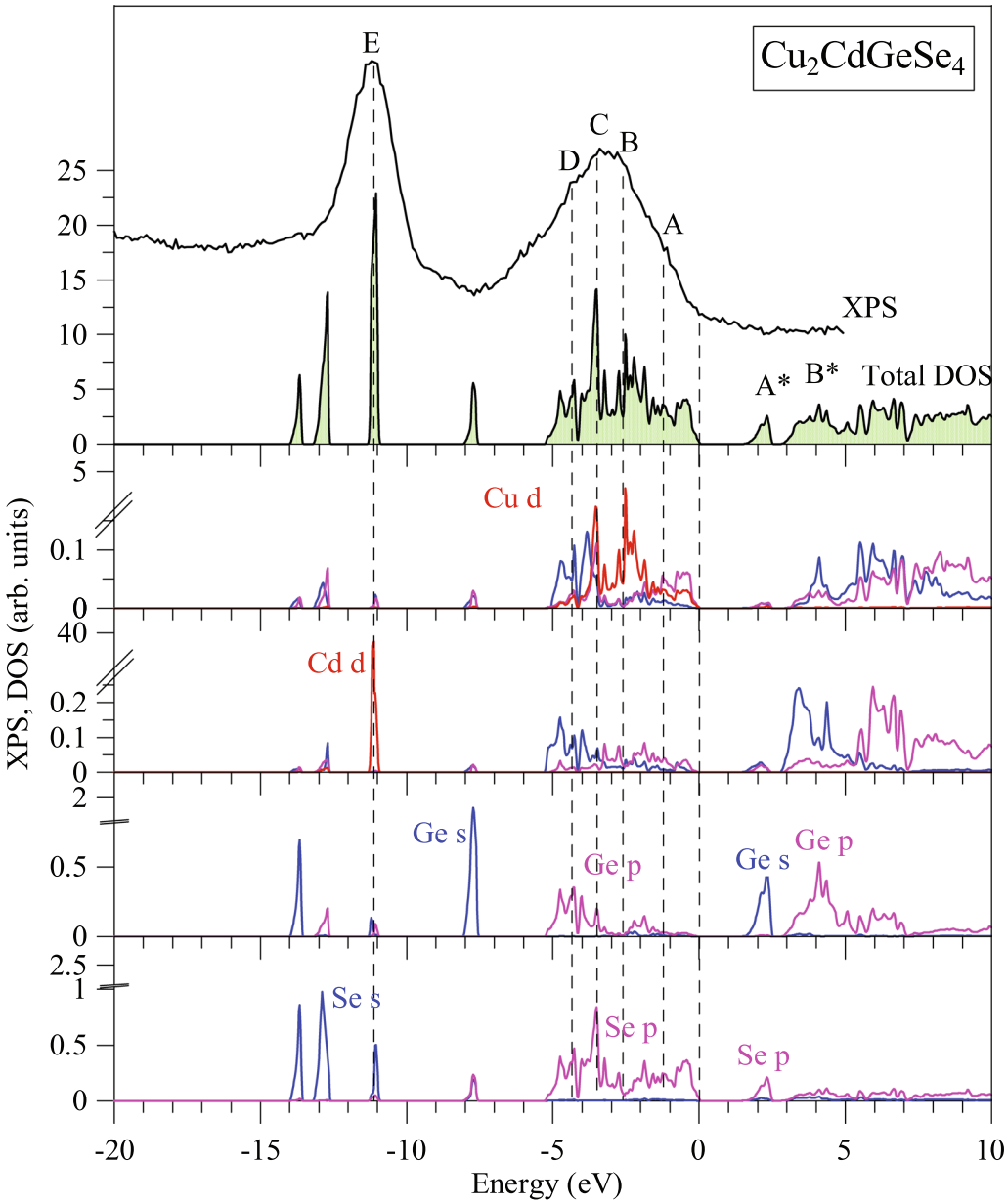

Fig. 5. Total DOS and PDOS of $Cu_2CdGeSe_4$ compound calculated within the mBJ + U method as compared to the XPS valence band spectrum measured in Ref. 11.

the chemical bonding of $Cu_2CdGeSe_4$. The energy shifts in the positions of the peaks associated with Cu 3*d* and Cd 4*d* states were by approximately 0.6 eV and 2.1 eV away from the Fermi energy level, which makes them consistent with the C and E peaks on the XPS spectrum when the GGA + U and mBJ + U methods are applied. The reason for this shift is that when the *U* value is added, the significant interaction of Cu 3*d* and Cd 4*d* electrons is taken into account.

The two-dimensional map of electron density of the $Cu_2CdGeSe_4$ model used is shown in Fig. 6 with the following planes: (1 – 1 0), as in Fig. 6a, and (– 1 1 0), as in Fig. 6b. The black contour lines are presented for electron densities from 0 e/Bohr^3 to 0.1 e/Bohr^3 with the interval of 0.01 e/Bohr^3. Figure 6a and b shows the spatial regions between the pairs of Cd-Se, Cu-Se and Ge-Se atoms with electron densities of 0.06 e/Bohr^3, 0.07 e/Bohr^3 and 0.09 e/Bohr^3, respectively. These spatial regions are formed by the orbital overlap of Cd, Cu and Ge atoms with Se atoms that represents the covalent component of the Cd-Se, Cu-Se and Ge-Se bonds in the $Cu_2CdGeSe_4$ crystal.

The band gap values calculated by using the different approximations are given in Table II. It can be seen that the GGA method underestimates the band gap of semiconductors and insulators.[28] The band gap obtained by the APW + lo calculations using the GGA approximation is equal to 0.255 eV

which is very dissimilar to the experimental data (E_g = 1.29 eV) given by Mkrtchyan et al.[9] This increases to 0.553 eV when applying the GGA + U method. The E_g values are equal to 0.784 eV and 0.938 eV when applying the mBJ and YS-PBE0 approaches, respectively (Table II). The use of the mBJ + U approximation yields a band gap of 1.297 eV which coincides with the experimental data.[9] Our previous results have revealed that the mBJ + U approach is the most appropriate approximation for calculating the band gap values of halides and chacolgenides[24,29–35] and, from the above analysis, it can be concluded that it is best suited for calculating the electronic properties of $Cu_2CdGeSe_4$. This choice is consistent with previous theoretical studies.[36–40]

The band structure of the $Cu_2CdGeSe_4$ compound with different high-symmetry points is shown in Fig. 7. The coordinates of these points are listed as follows: Γ (0.0, 0.0, 0.0), *X* (0.0, 0., 0.5), *Y* (0.13522, 0.13522, 0.5), Σ (0.31761, 0.31761, 0.31761), Γ (0.0, 0.0, 0.0), *Z* (0.5, 0.5, 0.5), Σ_1 (0.31761, 0.68239, 0.31761), *N* (0.0, 0.5, 0.0), *P* (0.25, 0.25, 0.25), Y_1 (0.5, 0.5, 0.13522) and *Z* (0.5, 0.5, 0.5). Our DFT calculations indicate that the valence band maximum (VBM) and conduction band minimum (CBM) of the $Cu_2CdGeSe_4$ compound are located at the Γ point (0.0, 0.0, 0.0), revealing its direct band gap nature, as shown in Fig. 7a.

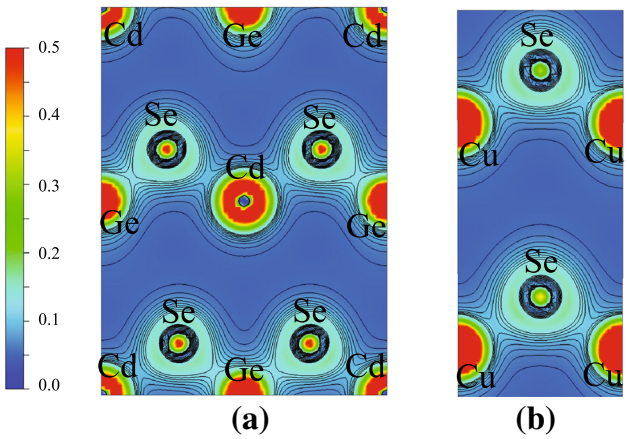

Fig. 6. Maps of electron density for the used $Cu_2CdGeSe_4$ model following the different planes: (a) (1 − 1 0) and (b) (− 1 1 0). The electron densities from 0 e/Bohr^3 to 0.1 e/Bohr^3 with the interval of 0.01 e/Bohr^3 stand for black contour lines.

Optical Properties

We further investigated the optical properties of the $Cu_2CdGeSe_4$ compound using the mBJ + U approximation. Note that the absorption coefficient $\alpha(\omega)$ is an important indicator for evaluating the applicability of materials in the field of photovoltaics. The variation of the $\alpha(\omega)$ curve as a function of the photon energy along the *xx* and *zz* directions is presented in Fig. 8. We found that the absorption begins upon reaching $E_g \geq 1.29$ eV leading to electron excitation from the VBM to the CBM. The absorption coefficient increases rapidly with increasing photon energy. At photon energy of 9.5 eV, the absorption coefficient reaches its maximum of about $150{\cdot}10^4$ cm^{-1}. In addition, one can observe that absorption of photon energy by $Cu_2CdGeSe_4$ is the strongest [$\alpha(\omega) > 10^4$ cm^{-1}] in the energy range of 1.29–27.20 eV. The $\alpha(\omega)$ curve in this range reveals several spectral peculiarities due to the electronic transitions. The wide absorption spectrum and high absorption coefficient of $Cu_2CdGeSe_4$ suggest that it is an alternative candidate for application in thin-film solar cells based on copper indium gallium selenide (CIGS).

Our calculated real and imaginary parts of the dielectric function of the $Cu_2CdGeSe_4$ compound as a function of photon energy are presented in Fig. 9. It should be noted that the imaginary part of the dielectric function is strongly dependent on the absorption spectrum, whereas the real part of the dielectric function determines the diffraction and reflectance behavior of the compound. The value of statistical dielectric constants was determined from Fig. 9a as follows: $\varepsilon_1^{xx}(0) = 6.829$ and $\varepsilon_1^{zz}(0) = 7.376$. In addition, the expression $\delta\varepsilon = \left(\varepsilon_0^{zz} - \varepsilon_0^{xx}\right)/\varepsilon_0^{tot}$[41] indicates the positive uniaxial anisotropy that is equal to 0.077. The real part of the dielectric function consists of five peaks corresponding to photon energy levels A (∼ 2.1 eV), B (∼ 3.5 eV), C (∼ 6.3 eV), D (∼ 7.0 eV) and E (∼ 9.2 eV). The emergence of these peaks in both the real and imaginary parts of the dielectric function is due to the transition of electrons from different states

Table II. Band gap (E_g) of the $Cu_2CdGeSe_4$ compound calculated by different DFT methods

	Exchange–correlation potential				
E_g (eV)	GGA	mBJ	GGA + U	mBJ + U	YS-PBE0
This work	0.255	0.784	0.553	1.297	0.938
Exp.			1.29,[9] 1.20[3]		
Other works			0.017[a], 0.020[b], 0.032[b]		

[a]Ref. 8. [b]Ref. 10.

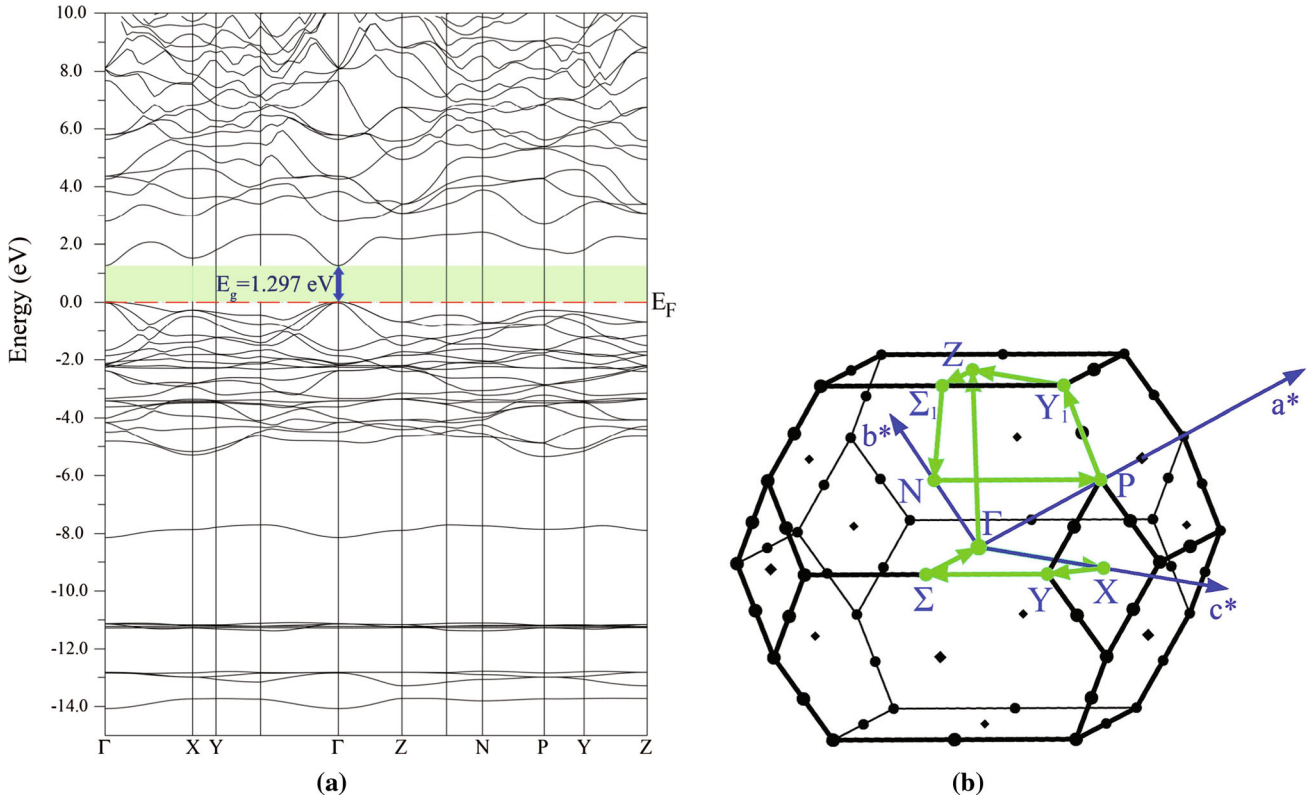

Fig. 7. (a) Electronic band structure and (b) diagram of the BZ for the tetragonal structure of the $Cu_2CdGeSe_4$ compound.

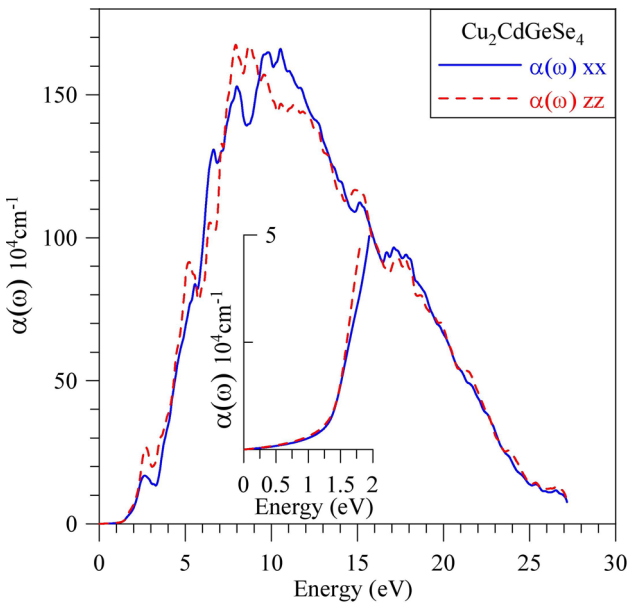

Fig. 8. Absorption coefficient $\alpha(\omega)$ of $Cu_2CdGeSe_4$ (calculated with mBJ + U).

within the VB to the states at the CB bottom. For example, from the position of the energy peaks in Figs. 5 and 9a, b, it can be deduced that peaks A (2.1 eV) and B (3.5 eV) are generated by electron transition from the valence states Cu 3*d* and Se 4*p* to the Ge 4*s* state of the CB. The peaks C (6.3 eV), D (7.0 eV) and E (9.2 eV) are generated by electron transition from the valence states Ge 4*p*, Se 4*p* and Cd 5*s* to the Ge 4*s* state of the CB. The interpretation of the origin of the peaks observed in the DFT calculations of the dielectric function includes only inter-band junctions taking into account the dipole selection rules for the matrix elements of the junction probabilities as it is suggested for such a case.[32] The present results of calculating the real and imaginary parts of the dielectric function within the mBJ + U approximation without the use of a scissor operator are consistent with those obtained by Brik et al.[10]

Figure 10 shows the dependence of the refractive index $n(\omega)$ (panel a), extinction coefficient $k(\omega)$ (panel b), electron energy-loss spectrum $L(\omega)$ (panel c), and optical reflection $R(\omega)$ (panel d) of $Cu_2CdGeSe_4$ on photon energy. Comparison of Figs. 9a and 10a shows similarities in the positions of the peak energy of the curve of the refractive index and the real part of the dielectric function. Calculated refractive indices of $Cu_2CdGeSe_4$ at zero frequency are $n^{xx}(0) = 2.613$ and $n^{zz}(0) = 2.716$ (Fig. 10a). The maximum value of $n(\omega)$ is detected within the photon energy range of 2–5 eV. Figure 10a shows that the $n(\omega)$ curve rapidly decreases with increasing photon energy at 5–15 eV, then it monotonously increases.

The extinction coefficient curve is similar to the curve of the imaginary part of the dielectric function

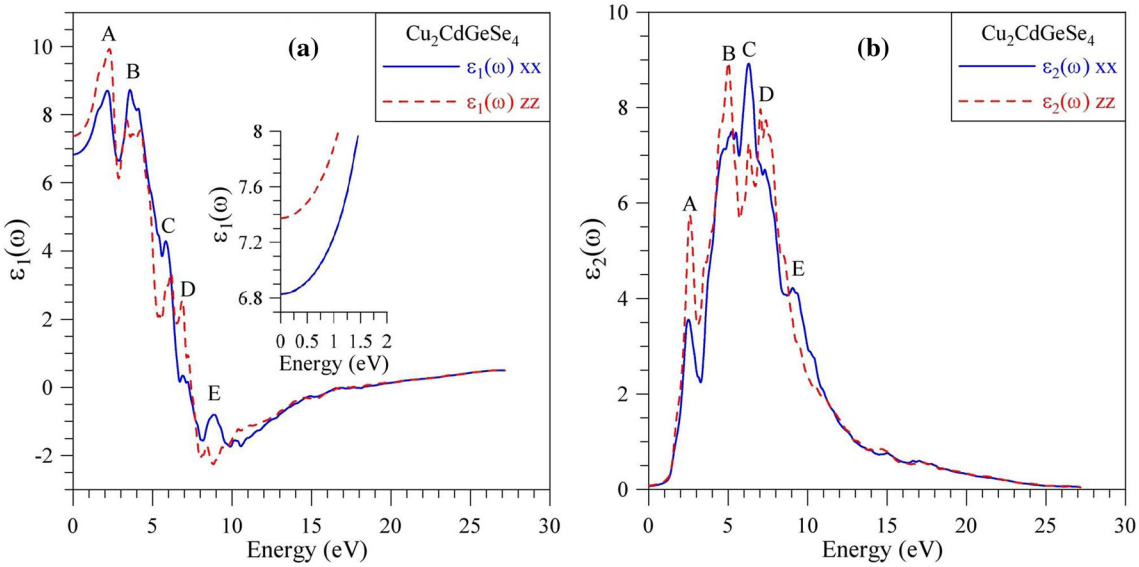

Fig. 9. (a) Real and (b) imaginary parts of the dielectric function [$\varepsilon_1(\omega)$ and $\varepsilon_2(\omega)$, respectively] of $Cu_2CdGeSe_4$ (calculated with mBJ + U). Note: two principal diagonal non-zero components of the second-rank dielectric tensor along the $\vec{a}$ and $\vec{c}$ axes are marked as *xx* and *zz*, respectively.

(Figs. 9b and 10b). The electron energy loss spectrum $L(\omega)$ characterizes the energy loss of electron beams due to inelastic scattering when propagated through solids.[42,43] Figure 10c shows that $L(\omega)$ starts with the photon energy value of the band gap (1.297 eV). $L(\omega)$ increases with ω reaching the maximum value when the photon energy is $\sim$ 20 eV and then rapidly decreases. Two components (in the directions x and z) of the optical reflectivity $R(\omega)$ at 0 eV are $R^{xx}(0) = 19.937\%$ and $R^{zz}(0) = 21.323\%$ (Fig. 10d). The optical reflectivity value increases with photon energy reaching the maximum value (44.243%) at the energy level of 8–12 eV and decreases with $\omega >$ 12 eV. Figure 10a–d shows that $Cu_2CdGeSe_4$ is anisotropic towards optical properties. This is a suitable feature of $Cu_2CdGeSe_4$ for the application of this material in thin-film solar cells and optoelectronic devices.

Elastic Properties

The elastic constants C_{11}, C_{12}, C_{13}, C_{33}, C_{44}, C_{66}, the G and E moduli and Poisson's ratio were calculated and discussed for the first time (Table III). The calculated value of the bulk modulus is in agreement with the results obtained previously by Brik et al.[10] The small values of elastic moduli B, E and G (Table III) of $Cu_2CdGeSe_4$ show that this material is less resistant to mechanical impact. The B-to-G ratio and the Cauchy pressure (C_{12}–C_{44}) are used to evaluate the ductile/brittle character of a material.[44,45] Accordingly, the material is ductile if the B-to-G ratio is larger than 1.75 and the Cauchy pressure is positive. For $Cu_2CdGeSe_4$, the B-to-G ratio = 2.74 and C_{12}–C_{44} = 33.6 GPa; it confirms high ductility of the $Cu_2CdGeSe_4$ compound. The ductility of $Cu_2CdGeSe_4$ also satisfies the criterion by Frantsevich[46] for Poisson's ratio of $\upsilon > 0.26$.

CONCLUSIONS

A systematic study of the structural, electronic, optical and elastic properties of $Cu_2CdGeSe_4$ was performed using the APW + lo method with different approximation functionals. Calculated results are compared to available experimental results and theoretical data.

Among the many different functionals used in the calculations (GGA, GGA + U, mBJ, mBJ + U), mBJ + U gives the best fit of calculated electron properties to the experimental data. This statement is supported by correspondence of the energy positions of the DOS energy peaks to the peak positions on the XPS valence band spectrum. Also, the band gap calculated in this study is E_g = 1.297 eV which is in good agreement with the experimental value [E_g(exp) = 1.29 eV]. The valence and conduction band extrema are located at the BZ Γ point (0.0, 0.0, 0.0) indicating that the $Cu_2CdGeSe_4$ compound is a direct gap material.

Typical optical constants such as the real $\varepsilon_1(\omega)$ and imaginary $\varepsilon_2(\omega)$ parts of the dielectric function, absorption coefficient $\alpha(\omega)$, refractive index $n(\omega)$, extinction coefficient $k(\omega)$, electron energy loss spectrum $L(\omega)$ and optical reflectivity $R(\omega)$ were calculated and discussed. The wide spectrum of absorbed photon energy (1.3–27.2 eV), high absorption coefficient (above 10^4 cm^{-1}) and optical

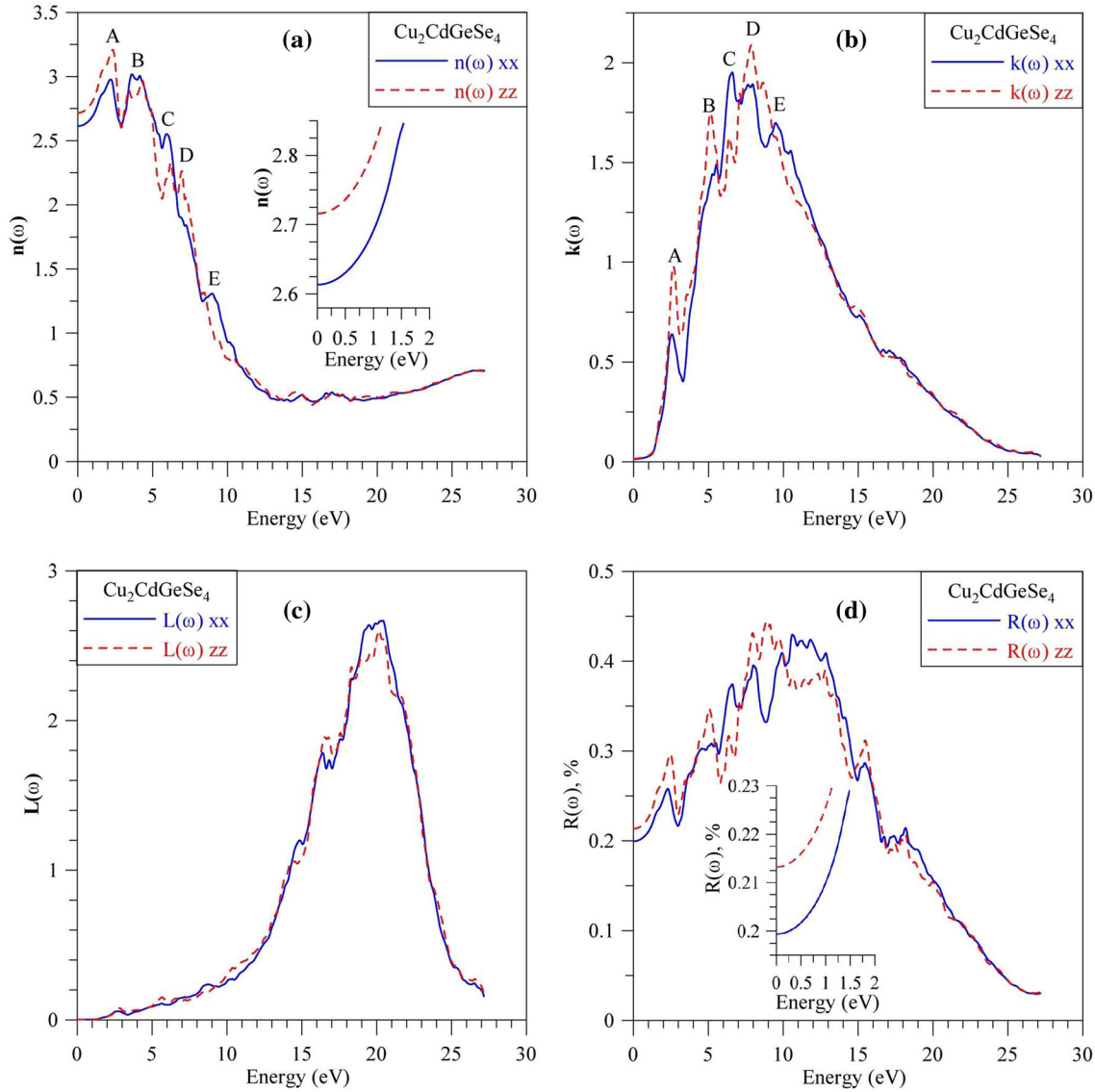

Fig. 10. (a) Refractive index $n(\omega)$, (b) extinction coefficient $k(\omega)$, (c) electron energy loss spectrum $L(\omega)$ and (d) optical reflectivity $R(\omega)$ of $Cu_2CdGeSe_4$ (calculated with mBJ + U). Note: two principal diagonal non-zero components of the secon- rank dielectric tensor along the $\vec{a}$ and $\vec{c}$ axes are marked as *xx* and *zz*, respectively.

Table III. Calculated values (on GPa) of elastic constants (C_{11}, C_{12}, C_{13}, C_{33}, C_{44}, C_{66}), bulk modulus (B), shear modulus (G), Young's modulus (E), Cauchy's pressure (C_{12}–C_{44}) and Poisson's ratio (υ) of $Cu_2CdGeSe_4$

C_{11}	C_{12}	C_{13}	C_{33}	C_{44}	C_{12}–C_{44}	C_{66}	B	G	E	υ
99.9	67.6	56.8	82.9	34.0	33.6	34.9	70.9 77[a10] 60[b10]	25.8	68.9	0.34

[a]Calculated using LDA. [b]Calculated using GGA.

anisotropy suggest useful application of $Cu_2CdGeSe_4$ in solar cell design. Furthermore, the compound can be applied in optoelectronic devices.

The elastic constants and moduli and the Poisson's ratio of $Cu_2CdGeSe_4$ were calculated using the Elastic software package. The results show that

$Cu_2CdGeSe_4$ is a highly ductile material with the B-to-G ratio of 2.74 and Poisson's ratio of 0.34. The elastic constants (C_{11}, C_{12}, C_{13},C_{33}, C_{44}, C_{66}), elastic moduli (G, E) and Poisson's ratio of $Cu_2CdGeSe_4$ were theoretically derived for the first time in this study.

REFERENCES

1. E. Parthe, K. Yvon, and R.H. Deitch, *Acta Crystallogr. B* 25, 1164 (1969).
2. L. Guen, W.S. Glaunsinger, and A. Wold, *Mater. Res. Bull.* 14, 463 (1979).
3. H. Matsushita, T. Maeda, A. Katsui, and T. Takizawa, *J. Cryst. Growth* 208, 416 (2000).
4. O.V. Parasyuk, L.V. Piskach, Y.E. Romanyuk, I.D. Olekseyuk, V.I. Zaremba, and V.I. Pekhnyo, *J. Alloys Compd.* 397, 85 (2005).
5. G.-Q. Yao, H.-S. Shen, E.D. Honig, R. Kershaw, K. Dwight, and A. Wold, *Solid State Ionics* 24, 249 (1987).
6. C. Wang, S. Chen, J.-H. Yang, L. Lang, H.-J. Xiang, X.-G. Gong, A. Walsh, and S.-H. Wei, *Chem. Mater.* 26, 3411 (2014).
7. L.D. Gulay, Y.E. Romanyuk, and O.V. Parasyuk, *J. Alloys Compd.* 347, 193 (2002).
8. D. Li, F. Ling, Z. Zhu, and X. Zhang, *Phys. B* 406, 3299 (2011).
9. S. Mkrtchyan, K. Dovletov, E.G. Zhukov, A. Melikdzhanyan, and S. Nuryev, *Neorg. Mater.* 24, 1094 (1988).
10. M.G. Brik, O.V. Parasyuk, G.L. Myronchuk, and I.V. Kityk, *Mater. Chem. Phys.* 147, 254 (2014).
11. V.A. Ocheretova, O.V. Parasyuk, A.O. Fedorchuk, and O.Y. Khyzhun, *Mater. Chem. Phys.* 160, 345 (2015).
12. Y. Zhang, Y. Wang, J. Zhang, L. Xi, P. Zhang, and W. Zhang, *J. Chem. Phys.* 144, 194706 (2016).
13. P. Blaha, K. Schwarz, G.K.H. Madsen, D. Kvasnicka, J. Luitz, R. Laskowski, F. Tran, and L.D. Marks, *WIEN2k, An Augmented Plane Wave + Local Orbitals Program for Calculating Crystal Propertie* (Wien: Techn. Universitat, 2018). ISBN 3-9501031-1-2.
14. J.P. Perdew and W. Yue, *Phys. Rev. B* 33, 8800 (1986).
15. J.P. Perdew, K. Burke, and M. Ernzerhof, *Phys. Rev. Lett.* 77, 3865 (1996).
16. J.P. Perdew, J.A. Chevary, S.H. Vosko, K.A. Jackson, M.R. Pederson, D.J. Singh, and C. Fiolhais, *Phys. Rev. B* 46, 6671 (1992).
17. F. Tran and P. Blaha, *Phys. Rev. Lett.* 102, 226401 (2009).
18. D. Koller, F. Tran, and P. Blaha, *Phys. Rev. B* 85, 155109 (2012).
19. F. Tran and P. Blaha, *Phys. Rev. B* 83, 235118 (2011).
20. V.I. Anisimov, I.V. Solovyev, M.A. Korotin, M.T. Czyzyk, and G.A. Sawatzky, *Phys. Rev. B* 48, 16929 (1993).
21. P. Novak, F. Boucher, P. Gressier, P. Blaha, and K. Schwarz, *Phys. Rev. B* 63, 235114 (2001).
22. P.E. Blochl, O. Jepsen, and O.K. Andersen, *Phys. Rev. B* 49, 16223 (1994).
23. A. Reshak, K. Nouneh, I. Kityk, J. Bila, S. Auluck, H. Kamarudin, and Z. Sekkat, *Int. J. Electrochem. Sci.* 9, 955 (2014).
24. T.V. Vu, A.A. Lavrentyev, B.V. Gabrelian, O.V. Parasyuk, V.A. Ocheretova, and O.Y. Khyzhun, *J. Alloys Compd.* 732, 372 (2018).
25. R. Golesorkhtabar, P. Pavone, J. Spitaler, P. Puschnig, and C. Draxl, *Comput. Phys. Comm.* 184, 1861 (2013).
26. R. Hill, *Proc. Phys. Soc. A* 65, 349 (1952).
27. R. Hill, *J. Mech. Phys. Solids* 11, 357 (1963).
28. J. Heyd, J.E. Peralta, G.E. Scuseria, and R.L. Martin, *J. Chem. Phys.* 123, 174101 (2005).
29. A.A. Lavrentyev, B.V. Gabrelian, V.T. Vu, P.N. Shkumat, V.A. Ocheretova, O.V. Parasyuk, and O.Y. Khyzhun, *Opt. Mater.* 47, 435 (2015).
30. T.V. Vu, A.A. Lavrentyev, B.V. Gabrelian, V.A. Ocheretova, O.V. Parasyuk, and O.Y. Khyzhun, *Mater. Chem. Phys.* 208, 268 (2018).
31. A.A. Lavrentyev, B.V. Gabrelian, V.T. Vu, L.N. Ananchenko, L.I. Isaenko, A.P. Yelisseyev, and O.Y. Khyzhun, *Opt. Mater.* 66, 149 (2017).
32. T.V. Vu, A.A. Lavrentyev, B.V. Gabrelian, O.V. Parasyuk, and O.Y. Khyzhun, *Mater. Chem. Phys.* 219, 162 (2018).
33. B.V. Gabrelian, A.A. Lavrentyev, T.V. Vu, O.V. Parasyuk, and O.Y. Khyzhun, *Opt. Mater.* 75, 538 (2018).
34. T.V. Vu, A.A. Lavrentyev, B.V. Gabrelian, O.V. Parasyuk, and O.Y. Khyzhun, *J. Electron. Mater.* 47, 5525 (2018).
35. A.A. Lavrentyev, B.V. Gabrelian, T.V. Vu, P.N. Shkumat, P.M. Fochuk, O.V. Parasyuk, I.V. Kityk, I.V. Luzhnyi, O.Y. Khyzhun, and M. Piasecki, *Inorg. Chem.* 55, 10547 (2016).
36. A.H. Reshak, *Appl. Catal. B* 225, 273 (2018).
37. D.P. Rai, Sandeep, A. Shankar, R. Khenata, A.H. Reshak, C.E. Ekuma, R.K. Thapa, and S.-H. Ke, *AIP Adv.* 7, 045118 (2017).
38. R. Jaradat, M. Abu-Jafar, I. Abdelraziq, S.B. Omran, D. Dahliah, and R. Khenata, *Mater. Chem. Phys.* 208, 132 (2018).
39. S.F. Solodovnikov, V.V. Atuchin, Z.A. Solodovnikova, O.Y. Khyzhun, M.I. Danylenko, D.P. Pishchur, P.E. Plyusnin, A.M. Pugachev, T.A. Gavrilova, A.P. Yelisseyev, A.H. Reshak, Z.A. Alahmed, and N.F. Habubi, *Inorg. Chem.* 56, 3276 (2017).
40. Sandeep, D.P. Rai, A. Shankar, M.P. Ghimire, R. Khenata, S. Bin Omran, S.V. Syrotyuk, and R.K. Thapa, *Mater. Chem. Phys.* 192, 282 (2017).
41. G. Boyd, H. Kasper, and J. McFee, *IEEE J. Quantum Electron.* 7, 563 (1971).
42. S.L. Dudarev, G.A. Botton, S.Y. Savrasov, C.J. Humphreys, and A.P. Sutton, *Phys. Rev. B* 57, 1505 (1998).
43. A. Bouhemadou and R. Khenata, *Comput. Mater. Sci.* 39, 803 (2007).
44. S.F. Pugh, *The London, Edinburgh, and Dublin Philosophical Magazine and Journal of Science* 45, 823 (1954).
45. D.G. Pettifor, *Mater. Sci. Technol.* 8, 345 (1992).
46. I. Frantsevich, F. Voronov, and S. Bakuta, *Elastic Constants and Moduli of Elasticity of Metals and Non-metals* (Kyiv: Naukova Dumka, 1982).